THERMAL CYCLING SIMULATION DURING REMELTING PROCESS OF THE STEEL ASTM A743-CA6NM

Camila Almeida Martins
Jhon Jairo Ramirez-Behainne
Universidade Tecnológica Federal do Paraná - Av. Monteiro Lobato, s/n - Km 04 CEP 84016-210 - Ponta Grossa, PR, Brazil
cah.amartins@gmail.com, jhon@utfpr.edu.br

Abstract. *This study aimed to model numerically the thermal cycling resulting from the steel ASTM A743-CA6NM remelting process, as well as the temperature distribution during the cooling of the test body. The problem was solved with the support of the commercial software ANSYS / FLUENT ® 14.5 for the three-dimensional case using the finite volume method. The following simplifying assumptions were adopted: heat loss by natural convection, absence of radiation, no phase change, concentrated heat source, and thermophysical properties independent of temperature. The results were analyzed for two different current intensities: 90A and 130A, and compared with experimental measurements. The peak temperatures of the thermocouples near the fusion line for the current of 130A were well represented by the numerical model, with a maximum deviation of 9.62%. In the case of the more remote thermocouples from the fusion line, the best results were obtained for the current of 90A, not exceeding 5% of deviation. In general, it was found that the test body is heated and cooled faster than in the simulations. This can be considered as a consequence of the simplification in material properties, assumed constant with respect to temperature. The results of this study demonstrate that, given the adopted simplifications, the numerical model was able to satisfactorily reproduce the experimentally measured thermal cycles.*

Keywords*: Thermal Cycling, Remelting Process, Numerical Simulation, Finite Volume Method*

1. INTRODUCTION

Welding is one of the most important material-joining processes widely used in industry, being used in the manufacture of various components and structures, as well as restoration of damaged or worn parts. Currently, new techniques are being developed to reduce the disadvantages of welding processes. One of these techniques is thermal spraying, followed by coating remelting. The remelting process affects the coating and the base metal, creating a heat-affected zone (HAZ) as a result of the large amount of heat transfer, which profoundly affects weld pool solidification and microstructure. As the microstructural changes and residual stresses reflect the mechanical properties of the material, the study of temperature distribution during the process has attracted interest due to the possibility of controlling these changes to obtain a defect-free structure.

The simulation of the welding process was first studied analytically by Rosenthal (1946) in one, two and three dimensional heat flow settings and transient and permanent regimes. The author assumed constant physical properties, negligible heat losses, absence of phase changes, concentrated heat source and infinite medium. Despite the adopted simplifications, the Rosenthal equations were also taking into account in many works, such as in that presented by Wells (1952), who predicted the geometry of the weld pool and Adams (1958), who has derived analytical expressions for the cooling rate and temperature peak. Other studies show the use of finite difference method, such as in the work of Chuansong et al. (1993), and Kim and Basu (1998), and the use of finite element method, presented by Wahab and Painter (1997) and Hong et al. (1998).

Wahab et al. (1998) developed two and three dimensional models using finite element method to determine the cooling time, weld penetration and width of weld pools. The results were compared with experimental measurements. Within a range of welding parameters, the results showed satisfactory agreement. Fassani (2001) developed analytical and numerical models for one- and two-dimensional configurations in transient regime, and also the settings for two- and three-dimensional in quasi-stationary regime for the simulation of multi-pass welding process. The author analyzed the losses by convection and radiation and the effect of the physical properties variation with temperature. Gery et al. (2005) presented a model of a moving distributed heat source based on the Goldak et al. (1984) double ellipsoid method. The effects of changes in welding parameters and the temperature distributions were analyzed. More recently, Attarha and Sattari-Far (2011) simulated three-dimensional models using the finite element method, and compared the numerical results to the experimental ones, obtaining a good agreement between them.

This study aimed to numerically model the temperature distribution (thermal cycling) in STEEL ASTM A743-CA6NM remelting process of for two different current intensities and subsequent cooling of the test body. The Finite Volume Method was applied with the support of the computational tool ANSYS / FLUENT ® 14.5 for the three-dimensional case.

2. MATERIALS AND METHODS

The simulated prototype was a 50mm wide, 25mm high and 75mm length body test. The remelting process in this geometry was studied experimentally by Oliveira (2011), who evaluated the influence of parameters, such as continuous or pulsed current and current intensity on the thermal cycle originated during the thermal spraying process on steel ASTM A743 CA6NM followed by plasma remelting. In this study, 11 thermocouples were fixed in the test body in order to map multiple active cycles during remelting.

Figure 1 shows the thermocouples position, indicating its coordinates (x,y,z) in mm.

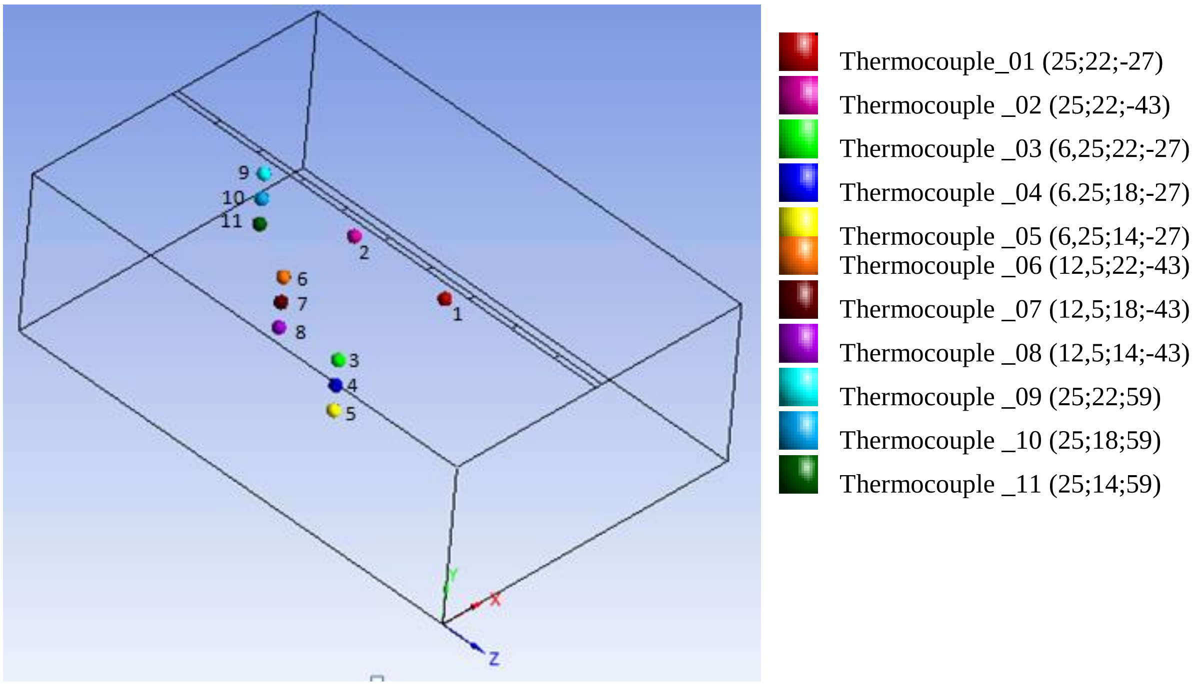

Figure 1. Thermocouples position

The welding process is treated as a heat source moving along the weld line. The analysis was performed on a central pass welding and it was estimated a 0.15 mm width application zone along the length of the test body. To simulate the movement of the weld, the application area was subdivided into 20 surfaces, so that, after a certain time, the source stops being applied to a surface and shall be applied in the following one.

Two boundary conditions are considered in the simulation. The first one is the thermal flow at the fusion line and the second one is the heat loss by natural convection in the other exposed surfaces of the sample. The following simplifying assumptions were adopted for the study: heat loss by natural convection, absence of radiation, no phase change, concentrated heat source and thermophysical properties independent of temperature.

The assumption of heat loss by natural convection becomes relevant in this problem, since this significantly influences the cooling rate, the peak temperature and the temperature distribution (JHAVERI et al., 1962).

In addition, the latent heat associated with the phase change was no considered significant for this study. The latent heat effects are more significant on weld bead morphology and weld pool size research. According Fassani (2001), the amount of energy stored in the melt pool due to phase change is negligible when compared to the initial heat input (around 2%).

It is known the material thermal conductivity and specific heat vary with respect to temperature. As the welding process involves high temperature gradients, these properties changes become clearly more significant. However, lack of data and of behavioral curves describing the ASTM A743 CA6NM properties variation with temperature, justifies the use of constant thermophysical properties.

The finite volume method was applied using the computational tool ANSYS / FLUENT ® 14.5. The simulations were performed on a computer with Intel ® Core i7-3612QM CPU 2.10 GHz processor with 8 GB of RAM. The average simulation time ranged around 2.5 seconds for each welding source position.

The finite volume mesh was refined near the fusion line, where the temperature gradients are larger. The mesh has 20,492 hexahedral and tetrahedral elements and 18,450 nodes, and it was defined after a mesh test.

The process parameters are described in Table 1.

Table 1. Process parameters used in simulations

Current	90 A	110 A	130 A
Voltage	17 V		
Efficiency	0,6		
Welding speed	10 cm/min		
Heat flux	$81{,}60 \times 10^6$ W/m^2	$99{,}73 \times 10^6$ W/m^2	$176{,}80 \times 10^6$ W/m^2
Convection heat transfer coefficient	5 W/m2K		
Time step (Welding)	0,25 s		
Time step (Cooling)	1,00 s		
Maximum number of iterations per time step	100		
Transient formulation	First order – Implicit		

To simulate the welding speed of 10 cm/min (0.00167 m/s), the heat source was applied for 2.25 seconds on each one of the 20 subdivisions of welding application area. Initially, the thermal flux was applied in the first melting line subdivision, and natural convection was applied on the other areas. After the convergence of the results, the boundary conditions were manually modified. Thus, the results of the previous simulation were used as initial conditions for the next one. The heat flow was then applied on the second subdivision, and natural convection was considered on the other areas. The same procedure was repeated for the 20 subdivisions, simulating the movement of the welding source.

The test body was preheated to a temperature of 150 °C. Two different electric current intensities were used in the simulations: 90A ($8{,}16 \times 10^7$ W/m^2) and 130A ($17{,}68 \times 10^7$ W/m^2).

The cooling simulation was also performed using as initial condition the welding simulation results. Then, the natural convection boundary condition was applied on all surfaces. The test body was cooled for 300 seconds.

3. RESULTS AND DISCUSSIONS

Figure 2(a-d) illustrates the temperature distribution for a current of 110A, along the ZX plane located 3mm from the fusion line. Figure 2(a) illustrates the initial stage of the process in which the heat source is applied to the first melting line subdivision. The source movement is shown in Fig. 2(b-d).

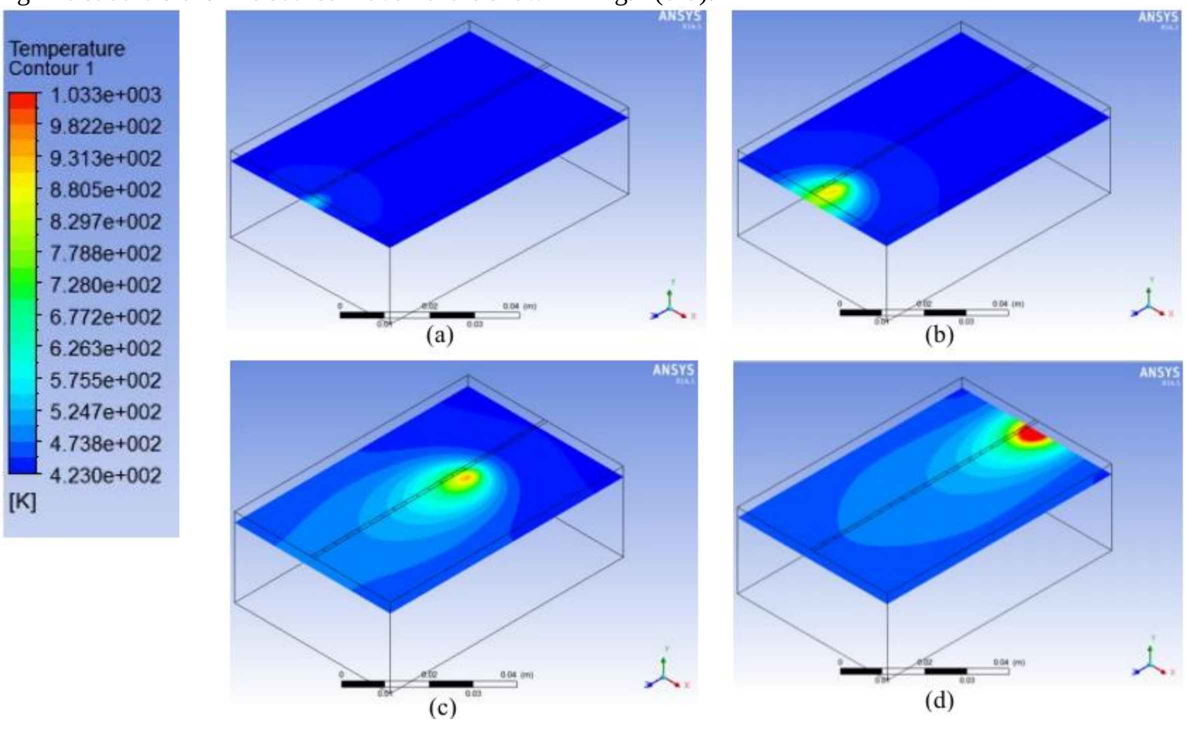

Figure 2. Temperature distribution during the welding process with a current of 110A after (a)0,25s (b)5s (c)30s (d)45s

3.1 Continuous current 90A

Figure 3 illustrates the temperature distribution (thermal cycling) obtained using the 90A current (Fig. 3-a) compared with the experimental results from Oliveira (2011) (Fig. 3-b).

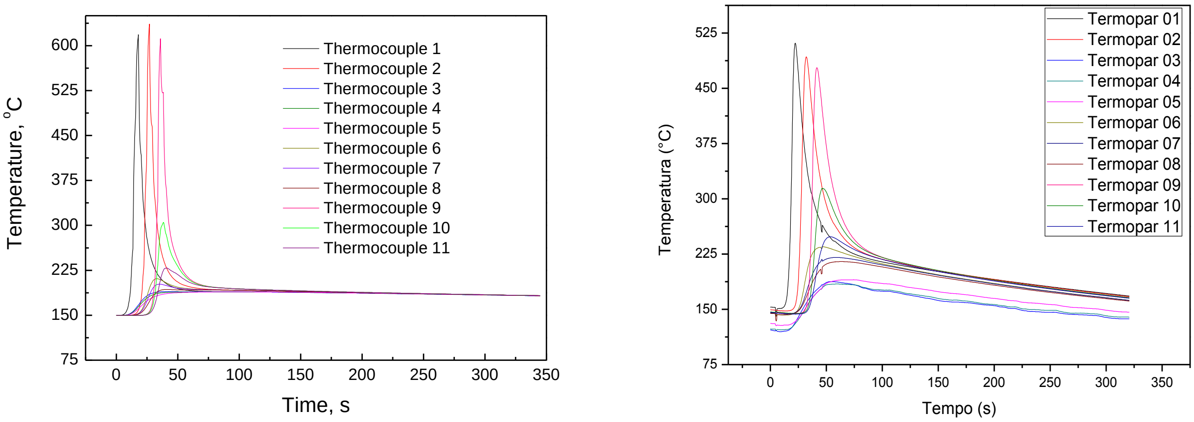

(a) (b)

Figure 3. Temperature distribution obtained using the 90A current intensity (a) Simulations (b) Experimental

The simulated behavior is similar to those based on experimental data. For the 90A continuous current, the greatest temperature differences were found near the fusion line (from 13.83% to 19.45%). For the more remote thermocouples from the fusion line, the results get closer to experimental data, not exceeding 5% of deviation, which can be considered a satisfactory result taking into account the simplifications adopted to solve the problem.

3.3 Continuous current 130A

Figure 4 illustrates the temperature distribution (thermal cycling) obtained using the 130A current (Fig. 4-a) compared with the experimental results from Oliveira (2011) (Fig. 4-b).

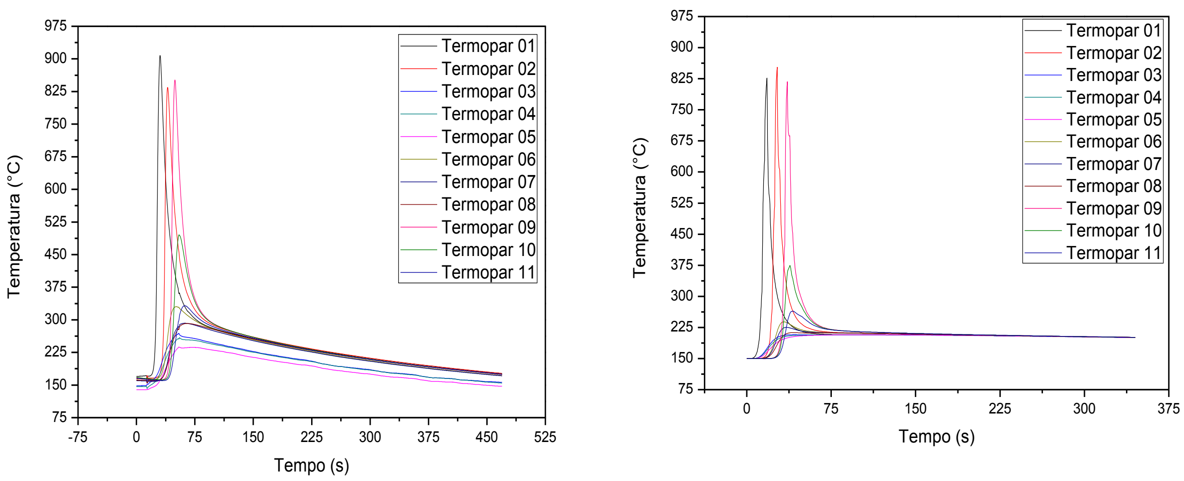

(a) (b)

Figure 4. Temperature distribution obtained using the 130A current intensity (a) Simulations (b) Experimental

For the current of 130A, deviations ranged from 3.43% to 9.62% at the thermocouple near the fusion line. For those more distant from the fusion line, deviations became more significant, ranging from 5 74% to 17.85%. It is interesting to note that at this current intensity, the time period needed for attaining the peak temperature decreased compared to the 90A current, again is a result of the higher thermal energy used in the process.

3.4 Peak temperatures analysis

Figure 5 shows the peak temperatures obtained at Thermocoupes 9, 10 and 11, along the Y-axis (25mm deep).

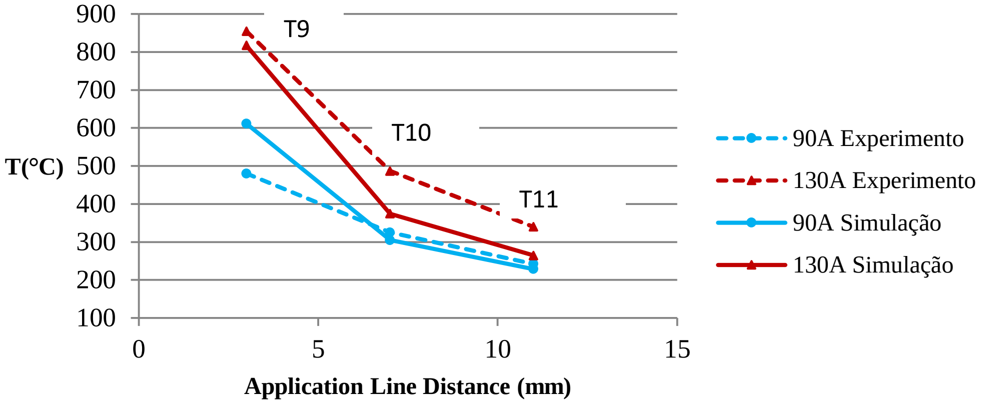

Figure 5. Peak temperatures obtained at Thermocouples 9, 10 e 11 along Y-axis

Comparing the peak temperatures obtained by simulation and the experimental results, it is noted that both have the same behavior. In general, the closer are the thermocouples to the fusion line (3mm), the lower are the deviation between the simulation and the experimental results. For the 90A current, it is noted that the simulated temperature at Thermocouple 9 is much higher than the experimental temperature. However, they approach quickly as the thermocouples move away from the fusion line.

Figure 6 shows the peak temperatures obtained at Thermocouples 6, 7 and 8, along the Y-axis (12.5mm deep).

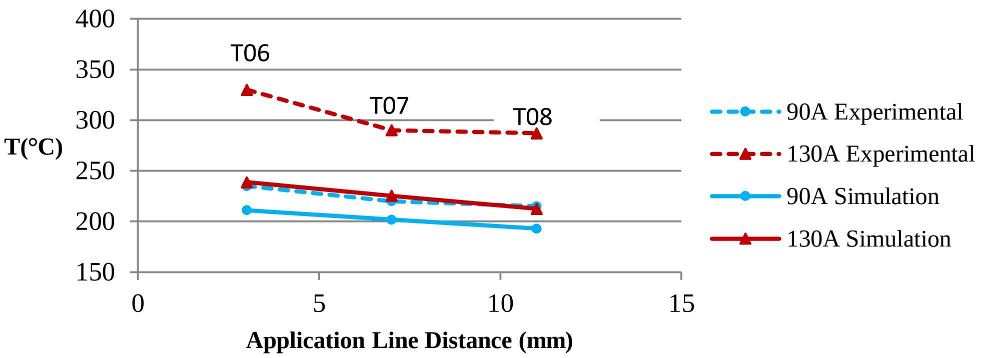

Figure 6. Peak temperatures obtained at Thermocouples 6, 7 e 8 along Y-axis

Analyzing the experimental results, it is observed that, for all the thermocouples, the temperature decrease is within the expected behavior.

Figure 7 shows the peak temperatures obtained at Thermocouples 3, 4 and 5, along the Y-axis (6.25mm deep).

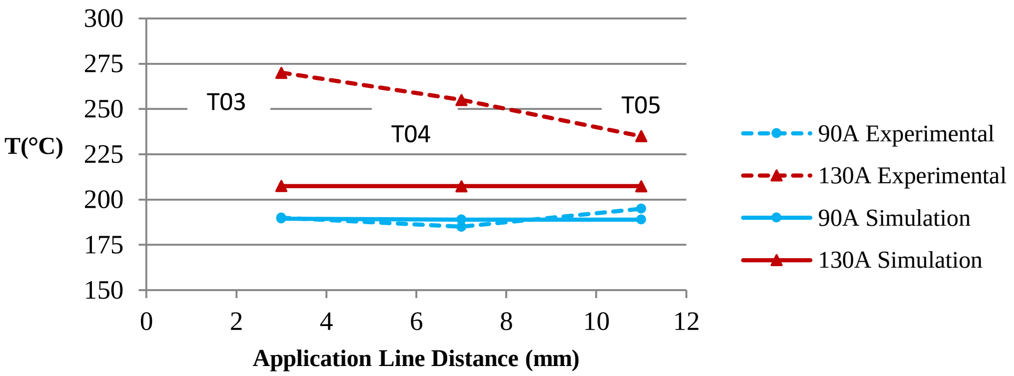

Figure 7. Peak temperatures obtained at Thermocouples 3, 4 e 5 along Y-axis

In Fig. 7, the simulated temperatures are almost constant, while the specimen still cooling, thereby confirming the analysis done on Fig. 6.

For both current intensities, the peak temperatures were obtained from the thermocouples along the z axis, close to the source application areas. Figure 8 shows the peak temperatures obtained at Thermocouples 1, 2 and 9.

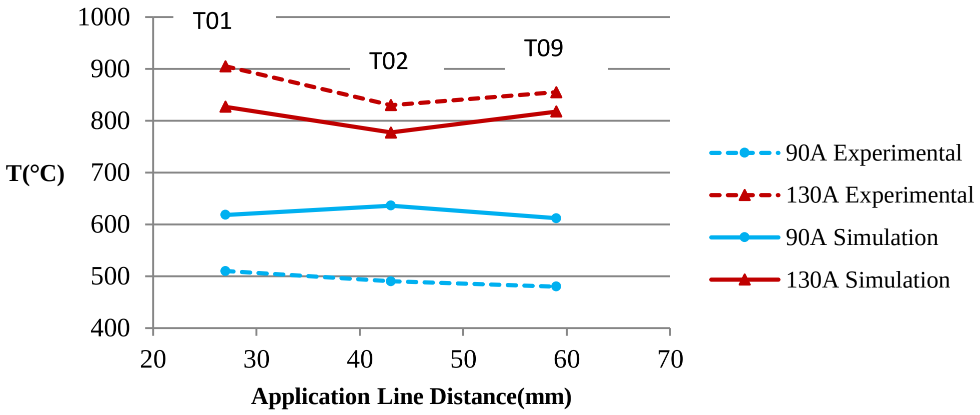

Figure 8. Peak temperatures obtained at Thermocouples 1, 2 and 9 along Z-axis

The analyzed thermocouples were located closer to remelting line (3mm in Y-axis) and varing only the Z distance (welding direction), thus having the highest peak temperature.

3.5 Cooling rate analysis

Figure 9(a-b) illustrates the temperature distribution during the specimen cooling process for a current of 110A, along the ZX plane located 3mm from the fusion line.

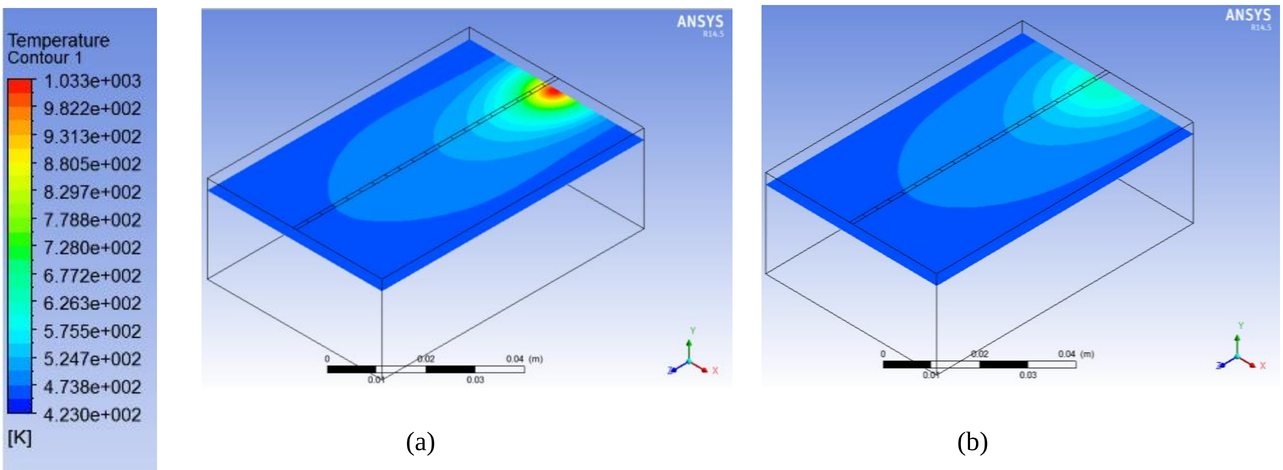

Figure 9. Temperature distribution during the cooling process for a current of 110A after (a) 46s (b)50s

In Figure 10 are shown the cooling curves obtained from Thermocouple 9, which was located 3mm from the fusion line. The curves started at the peak temperature and demonstrated the variation in cooling rate when changing the current intensity used in the process. The results obtained by simulation (Fig. 10-a) were compared with those obtained experimentally by Oliveira (2011) (Fig. 10-b). Breaks along the curves in Figure 10-a are due to the not continuous heat source movement during the simulations.

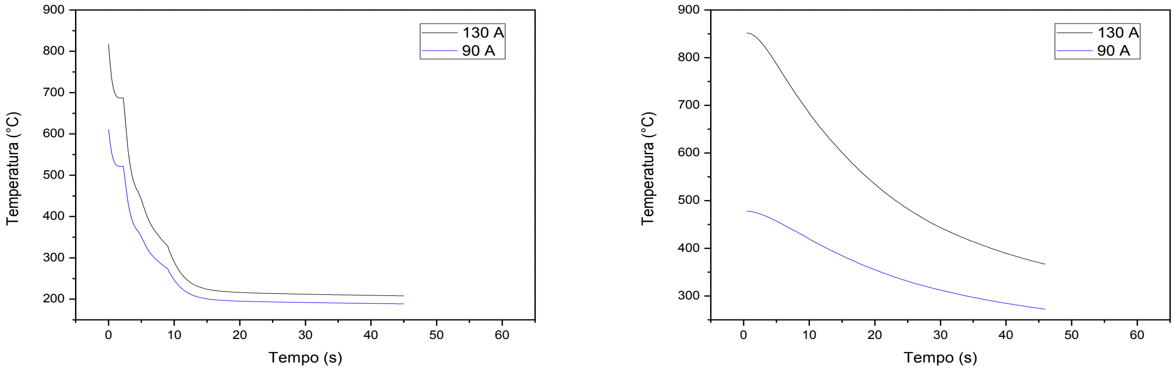

(a) (b)

Figure 10. Thermocouple 9 cooling curve, starting at peak temperature (a) Simulations (b) Experimental

In Fig. 11 sections of the Thermocouple 10 cooling curve, located 7mm from the fusion line, are presented. The results obtained by simulation (Fig. 11-a) were compared with those obtained experimentally by Oliveira (2011) (Fig. 11-b).

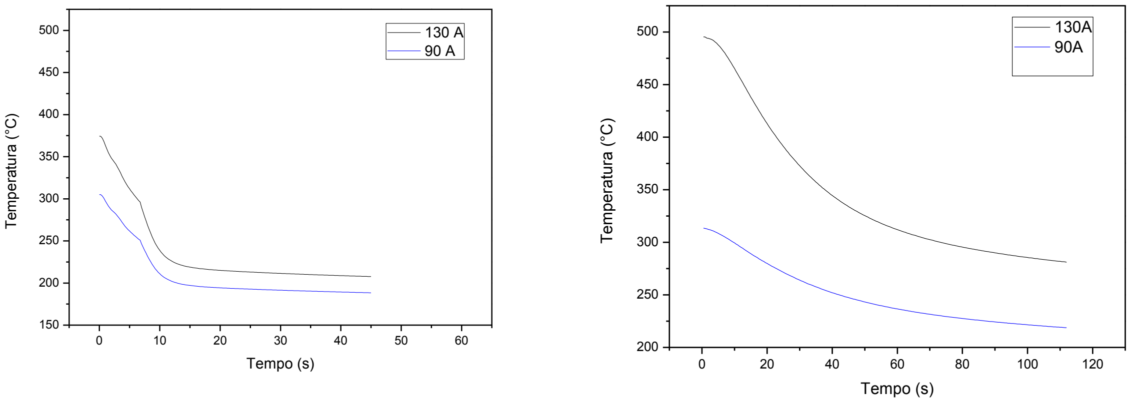

(a) (b)

Figure 11. Thermocouple 10 cooling curve, starting at peak temperature (a) Simulations (b) Experimental

The cooling rate for the thermocouples nearest the fusion line (Thermocouple 9) is greater than for the more distant ones. This can be explained by the fact that the peak temperature reached is greater for the thermocouples near the fusion line. In the most distant thermocouples, the cooling rate is slower, because the peak temperatures attained are reduced. However, due to the consideration of material properties constant with temperature, the same inclination isn't observed in the simulation results.

In Fig. 12 sections of the Thermocouple 11 cooling curve, located 1mm from the fusion line, are presented.

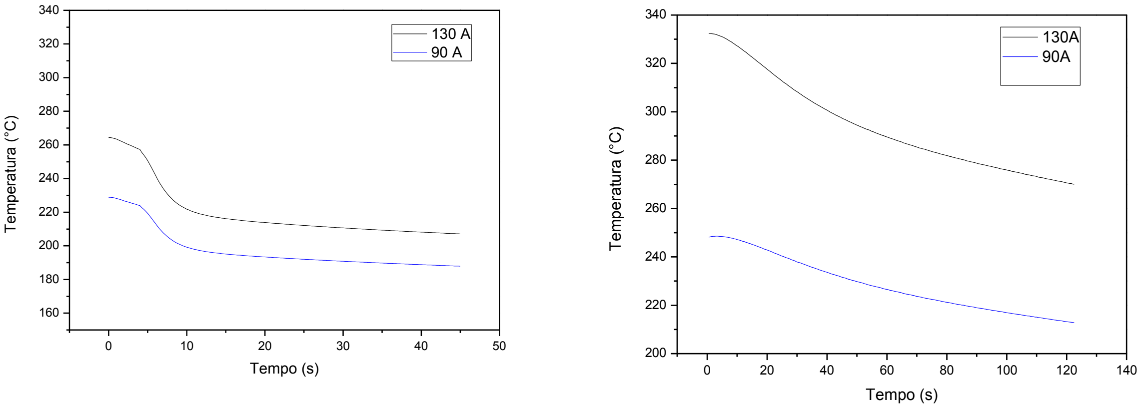

(a) (b)

Figure 12. Thermocouple 11 cooling curve, starting at peak temperature (a) Simulations (b) Experimental

Analyzing the results, it was found that cooling occurs faster in simulations. This can be justified by the consideration of constant thermophysical material properties, especially thermal diffusivity. It is also observed that, regardless of the intensity of current used, the cooling rate tends to stabilize over time.

The welding process creates high temperature gradients in the metal around the weld. In this case, the physical properties (thermal diffusivity) vary strongly and non-linearly with temperature. So, considering the thermophysical properties as constant can lead to considerable deviations. In simulations, the specific heat of steel was assumed constant at 430 J/kgK, which corresponded to 20 °C. Being verified that actually the specific heat of steel increases with the increasing of temperature, the heat capacity of the sample is higher than in the simulated cases, leading to heating and cooling times slower in comparison to those obtained in simulations.

4. CONCLUSIONS

In this study, it was possible to simulate and analyze the temperature distribution (thermal cycling) during the remelting process at two different current intensities. Despite the simplifying assumptions as no radiation, no phase change, concentrated heat source and thermophysical properties independent of temperature, in both cases, the simulated behavior was reasonable in comparisons with experimental data.

The approach used to solve the thermal welding problem proved to be applicable to engineering problems, since it is possible to determine, quickly and with low computational cost, the temperature field with an acceptable approximation to the experimental results. Thus, the results showed promise as an aid to remelting processes studies in which it is difficult to measure the temperature on specific locations of the sample.

5. ACKNOWLEDGEMENTS

The authors gratefully thank both the PROGRAD-UTFPR and the Campus Ponta Grossa for the financial support.

6. REFERENCES

Adams Jr, C. M.,1958. Cooling rates and peak temperatures in fusion welding. Welding Journal, Vol.37, n.5, pp. 210s-215s.

Attarh, M. J., Sattari-Far, I., 2011. Study on welding temperature distribution in thin welded plates through experimental measurements and finite element simulation. Journal of Materials Processing Technology, Vol.211, pp. 688-694.

Chuansong, W., Zhenning, C., Lin, W., 1993. Numerical analysis of three-dimensional fluid flow and heat transfer in TIG weld pool with full penetration. Acta MetallurgicaSinica, Series B, Vol.6, n.2, pp. 130-136.

Fassani, R. N. S., 2001. Modelamento Analítico e numérico da transferência de Calor no Processo de Soldagem com Múltiplos Passes. PhD. Thesis, Universidade Estadual de Campinas, Campinas, SP. Brazil.

Gery, D., Long, H., Maropoulos, P., 2005. Effects of welding seed, energy input and heat source distribution on temperature variations in butt joint welding. Journal of Materials Processing Technology, Vol.167, pp.393-401.

Goldak, J., Chakravarti, A. Bibby, M., 1984. A new finite element model for welding heat sources. Metallurgical Transactions B, Vol. 15B, pp.299-305.

Hong, K., Weckman, D. C., Strong, A. B., 1998. The influence of thermofluids phenomena in gas tungsten arc welds in high and low thermal conductivity metals. Canadian Metallurgical Quartely, Vol.37, n.3-4, pp.293-303.

Kim, I. S., Basu, A., 1998. A mathematical model of heat transfer and fluid flow in the gas metal arc welding process. Journal of Materials Processing Technology, Vol. 77, pp. 17-24.

Oliveira, F. R., 2011. Análise da influência dos parâmetros de refusão no ciclo térmico de revestimentos Fe-Cr-Mn-Si aspergidos e refundidos. Trabalho de Conclusão de Curso Bacharelado em Engenharia Mecânica, Universidade Tecnológica Federal do Paraná. Ponta Grossa, PR, Brazil.

Rosenthal, D., 1946. The theory of moving sources of heat and its application to metal treatments. Transactions of the American Society of Mechanical Engineers, Vol. 68, pp. 849 – 866.

Wahab, M. A., Painter, M. J., 1997. Numerical models of gas metal arc welds using experimentally determined weld pool shapes as the representation of welding heat source. International Journal of Pressure Vessels and Piping, Vol. 73, pp. 153-159.

Wahab, M. A., Painter, M. J., Davies, M. H., 1998. The prediction of the temperature distribution and weld geometry in the gas metal arc welding process. Journal of Materials Processing Thechnology, Vol. 77, pp.2333-239.

Wells, A. A., 1952. Heat Flow in Welding. Welding Journal, Vol..31, n.5, pp. 263s-267s.

7. RESPONSIBILITY NOTICE

The authors are the only responsible for the printed material included in this paper.